Nuclear Engineering and Technology 50 (2018) 68–79

Contents lists available at ScienceDirect

Nuclear Engineering and Technology

journal homepage: www.elsevier.com/locate/net

Original Article

Characteristics of regional scale atmospheric dispersion around Ki-Jang research reactor using the Lagrangian Gaussian puff dispersion model

Geun-Sik Choi [a], Jong-Myoung Lim [a], Kyo-Sun Sunny Lim [a], Ki-Hyun Kim [b], Jin-Hong Lee [c, *]

[a] Environmental Radioactivity Assessment Team, Korea Atomic Energy Research Institute, 111, Daedeok-daero 989, Yuseong-gu, Daejeon, 305-353, South Korea
[b] Department of Civil & Environmental Engineering, Hanyang University, 222, Wangsimni-ro, Seongdong-gu, Seoul 133-791, South Korea
[c] Department of Environmental Engineering, Chungnam National University, 220 Gung-dong, Yuseong-gu, Daejeon 305-764, South Korea

ARTICLE INFO

Article history:
Received 25 March 2017
Received in revised form
26 September 2017
Accepted 2 October 2017
Available online 28 October 2017

Keywords:
Atmospheric Dispersion of Radioactive Materials
California Puff
Ki-Jang Research Reactor
weather research and forecasting

ABSTRACT

The Ki-Jang research reactor (KJRR), a new research reactor in Korea, is being planned to fulfill multiple purposes. In this study, as an assessment of the environmental radiological impact, we characterized the atmospheric dispersion and deposition of radioactive materials released by an unexpected incident at KJRR using the weather research and forecasting–mesoscale model interface program–California Puff (WRF–MMIF–CALPUFF) model system. Based on the reproduced three-dimensional gridded meteorological data obtained during a 1-year period using WRF, the overall meteorological data predicted by WRF were in agreement with the observed data, while the predicted wind speed data were slightly overestimated at all stations. Based on the CALPUFF simulation of atmospheric dispersion (χ/Q) and deposition (D/Q) factors, relatively heavier contamination in the vicinity of KJRR was observed, and the prevailing land breeze wind in the study area resulted in relatively higher concentration and deposition in the off-shore area sectors. We also compared the dispersion characteristics between the PAVAN (atmospheric dispersion of radioactive release from nuclear power plants) and CALPUFF models. Finally, the meteorological conditions and possibility of high doses of radiation for relatively higher hourly χ/Q cases were examined at specific discrete receptors.

1. Introduction

The Ki-Jang research reactor (KJRR), a new research reactor in Korea with a 15 MW thermal power capacity, is being planned to fulfill multiple purposes. These include (1) advancing technology related to research reactors, (2) producing medical and industrial radioisotopes (e.g., Mo-99, I-131, and Ir-192), and (3) conducting neutron transmutation silicon doping to help meet growing global demand. The planned location for the KJRR is in a suburb of Busan City (35.3251 N, 129.2474 E) in the south-east region of South Korea. According to regulatory requirements, various assessments of the environmental radiological impacts have been carried out, including potential air dispersion release of radionuclides during an unexpected accident.

An accident at a nuclear facility like those that have occurred at Three Mile Island, Chernobyl, and Fukushima Daiichi can cause significant radioactive exposure on local, regional, and global scales. Thus, the importance of developing an emergency preparedness program when a new nuclear facility is planned and permitted is well recognized [1]. Emergency responses require instant information regarding the affected areas, the plume arrival times at critical locations, and the local scale of background radiation levels. To evaluate this and related information, an atmospheric dispersion model and high resolution meteorological field data with accurately estimated emission rates are mandatory for accurate prediction.

Several studies have been presented that have accurately estimated the affected areas and potential plume arrival times at critical locations following the Fukushima accident; in these studies, various air dispersion models were applied including the hybrid single-particle Lagrangian integrated trajectory, flexible

* *Corresponding author.*
E-mail address: jinlee@cnu.ac.kr (J.-H. Lee).

https://doi.org/10.1016/j.net.2017.10.002

particle dispersion model , system for prediction of environment emergency dose information, Lagrangian particle dispersion model, and California Puff model (CALPUFF) [2–8]. However, previous studies have identified the difficulties involved in accurately predicting the air dispersion of radioactive nuclides; these difficulties can result from uncertainties in the emission rates and the meteorological data [2,6]. For this reason, it is important to establish an accurate representation of temporally and spatially varying meteorological field patterns (e.g., temperature, humidity, wind direction, wind speed, vertical wind flow, radiation, mixing height, etc.) to simulate the transport and physicochemical dispersion of radioactive nuclides into the environment in the mesoscale area around nuclear facilities.

Gaussian straight line models such as XOQDOQ (meteorological evaluation of atmospheric nuclear power plant effluents) and PAVAN (atmospheric dispersion of radioactive release from nuclear power plants) are widely used to estimate air dispersion characteristics of radionuclides for the regulatory or permitting processes of a nuclear facility [9,10]. The results from these models tend to give the maximum dose in the study area. However, they have limited applicability while modeling a range of spatial and temporal scales. For this reason, for a local scale analysis (<10 km), Gaussian straight line models should be considered.

The CALPUFF model is a regulatory model defined by the United States Environmental Protection Agency (US EPA) that can be used to model complex wind regimes at local scale, as well as for modeling the regional transport of various pollutants [11]. Based on a tracer study, Rood (2014) pointed out that Lagrangian puff models such as CALPUFF may be preferably used for dose reconstruction for a large model domain [12]. The CALPUFF system can also be successfully used to evaluate dispersion characteristics for both real-time emergency response plans and long-term simulations. CALPUFF can be used with three-dimensional gridded meteorological fields to simulate mesoscale transport, dry–wet deposition, simple trajectories, and the decay of radioactive materials released from various types of time-integrated source terms (e.g., point, volume, area, and line). It has been used to estimate the dispersion of radioactive materials in several studies [13–15].

In this study, to evaluate the meteorological conditions and spatial regions of high-dose radiation exposure to the public, we attempted to characterize the atmospheric dispersion and deposition of radioactive materials released by an unexpected incident at KJRR. Also, a model system for realistic dispersion characteristics as a means of practical safety assessment for new research reactor was presented. For these main objectives, the weather research and forecasting (WRF) model from National Center for Atmospheric Research was used to produce high resolution meteorological fields. The meteorological model output from WRF was statistically compared to field measurement data in the study area. The atmospheric dispersion (χ/Q) and deposition (D/Q) factors, which correspond to the average concentration or deposition by using a unit release rate (Q), were calculated using three-dimensional gridded meteorological data collected during a 1-year study period using the weather research and forecasting–mesoscale model interface program–California Puff (WRF–MMIF–CALPUFF) model system. Finally, the meteorological conditions and spatial regions for high-dose radiation exposure to the public were examined at specific discrete receptors.

2. Methodology

2.1. Study area characteristics

The study area is located in the south-east of South Korea at 35.3°N and 129.2°E. KJRR is adjacent to large cities (e.g., Pusan and Ulsan) with more than 5,000,000 residents within a radius of 50 km. According to the 30-year monthly average of meteorological data measured by the Korea Meteorological Administration (KMA), the prevailing winds are from north and northeast directions. The average annual rainfall and temperature are about 1,500 mm and 14.5°C, respectively. As shown in Fig. 1, the topography of the study area is characterized generally as mountainous uplands about 150 m above sea level; the area has a complex coastline on the south and east sides. Therefore, the meteorology (especially, wind direction and speed) is significantly affected by thermal interactions between the mountains and the sea.

2.2. Field meteorology measurements

A meteorological station was installed at the north-east edge of the KJRR boundary (35.3251°N, 129.2474°E). The collected meteorological data, including wind speed, direction, temperature, pressure, and humidity at 65 m, 10 m, and 1.5 m, were recorded every 10 minutes beginning on 1 September 2014 and separately stored in a data logger (CR1000, Campbell). Additionally, hourly meteorological data (e.g., wind direction and speed) collected at weather observation stations in the modeling grid were extracted from the meteorological data archive of the KMA (available online at http://data.kma.go.kr/). The field measurement data and archive data in the modeling grid were then inputted and interpolated in the WRF model simulation to improve the prediction accuracy. To obtain the field measurement, the objective analysis technique (OBSGRID) provided by the WRF model was applied. By performing an objective analysis in meteorological modeling, we can improve meteorological analyses on the mesoscale grid by incorporating information from observations, and thus better model reproducibility can be expected [16].

2.3. WRF model simulation

WRF model, version 3.8.1 [17], which is a fully compressible nonhydrostatic model with an Arakawa-C grid system, was used to simulate the local meteorological fields around the study area. Since the simulation results of the meteorological fields are strongly dependent for numerical weather prediction on datum resolution and the initial meteorological analyses, the use of higher resolution geological datum is required to improve prediction accuracy [18,19]. Furthermore, integrating the observed meteorological field with data from surface and upper air measurements can also improve prediction accuracy [20].

The initial and boundary conditions were generated every 6 hours by the unified model–based regional data assimilation and prediction system in the KMA, with a horizontal resolution of 12 km (available online at http://data.kma.go.kr/). The low boundary for the model is based on the optimum interpolation sea surface temperature. The model simulation was started at 09:00 LST on 29 August 2014 and continued till 00 local standard time (LST) 1 September 2015. The analysis period excluded spin-up days during August 2014. One year of meteorological field data from 1 September 2014 to 1 September 2015 were evaluated and used as input for the dispersion model. As presented in Fig. 1, the model domain consists of one-way interactive triple nested domains with a Lambert conformal map projection. A 1-km domain covering the south-east part of the Korean peninsula, centered on KJRR (Domain 3, 142 × 142), is nested in a 3-km domain (Domain 2, 145× 145), which in turn is nested in a 9-km domain (Domain 1, 116× 132). All of the domains have 34 vertical layers with terrain following sigma coordinates, and the model top is 50 hPa. Note that the cumulus parameterization scheme is not used in the 1-km grid model, for which convective rainfall generation is assumed to be explicitly

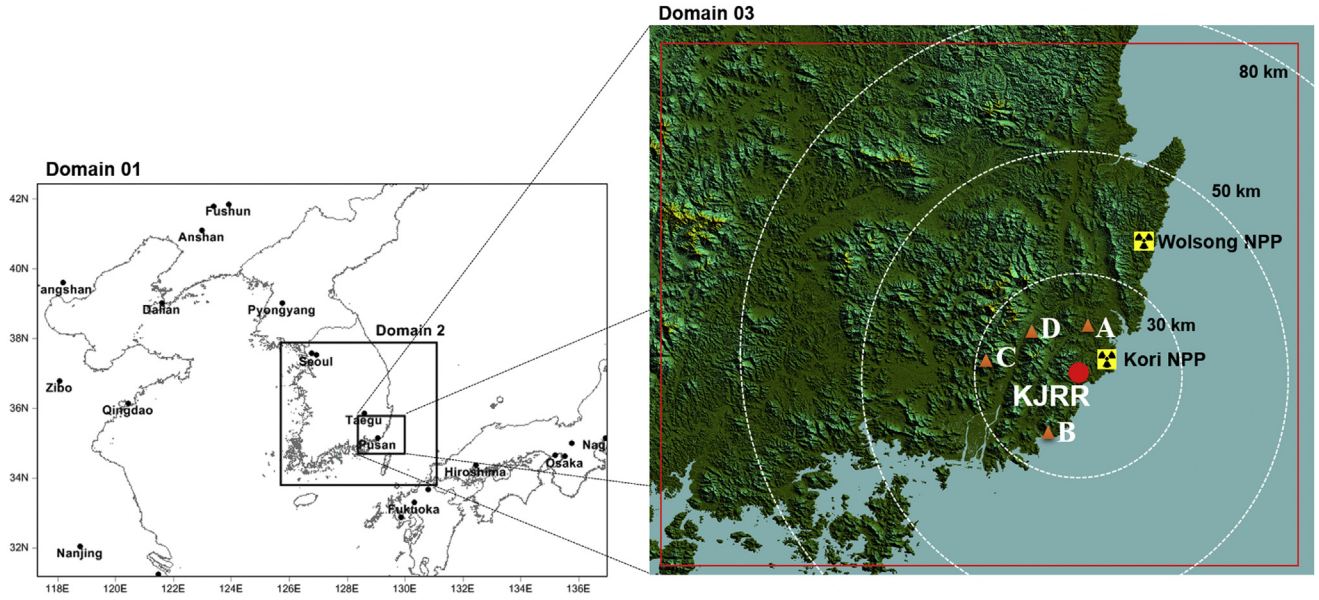

Fig. 1. Three nested domains used for WRF simulation (left). The right figure shows the location of KJRR and topography in the finest domain. The red line indicates the domain boundary of the CALPUFF simulation model. The automatic weather stations around 30 km radius of KJRR are indicated by red triangles; (A) Ulsan, (B) Busan, (C) Kimhae, and (D) Yangsan. (For interpretation of the references to color in this figure legend, the reader is referred to the web version of this article.)

resolved. To improve the prediction accuracy of the WRF model, high-resolution input data for the geological parameters (e.g., 90 m resolution (3s) obtained from the shuttle radar topography mission data from the National Aeronautics and Space Administration and a 30 m resolution medium division land cover map from the Korea Ministry of Environment, http://egis.go.kr) were used in the finest nested domain. The details of the physics and grid configuration in the WRF and modeling conditions in CALPUFF are summarized in Table 1.

2.4. CALPUFF model simulation

The CALPUFF modeling system is a multilayer, multispecies non–steady state Lagrangian Gaussian puff dispersion model that simulates the three-dimensional spatial and temporal transport, transformation, and deposition of a species [21]. The modeling system is currently the US EPA's preferred long-range dispersion model and is composed of three main modules: CALMET, CALPUFF, and CALPOST. CALMET, the meteorological module, generates geophysical data and a three-dimensional hourly gridded wind field and meteorological data. CALPUFF is the main module for simulating complex terrain effects, overwater transport, coastal interaction effects, building downwash, wet and dry removal, simple chemical transformation, and the decay of radionuclides. CALPOST is a postprocessing module that display the CALPUFF output in graphical form [11].

The parameters and direct input format of the CALPUFF dispersion module were extracted by the MMIF (v3.3) from the prognostic meteorological model output of the WRF [22]. The data for topographic height and land use, which play critical roles in the dispersion of pollutants, were also directly extracted by the MMIF. The model domain for long-term simulation was 131 × 131 grid units with a horizontal resolution of 1-km. The grid was covered after trimming five points off each edge of the WRF modeling domain. The vertical layers were divided into 10 levels with EPA/FLM (Federal Land Manager) guidance layers of 0, 20, 40, 80, 160,

Table 1
Details of the physics and grid configuration in the WRF and modeling conditions in CALPUFF.

Meteorological/dispersion models	WRF			CALPUFF	
Domains	Domain 1	Domain 2	Domain 3	Main domain	
Horizontal resolution	9 km	3 km	1 km	1 km	
Vertical levels	34	34	34	10	
Grid	116 × 132	145 × 145	142 × 142	131 × 131	
Domain center	38.0 N, 126.3 E			35.6 N, 128.8 E	
Initial/boundary conditions	RDAPS-based UM, KMA (12 km resolution)			Map projection	LCC
				Datum	WGS-84
Physics				*Conditions*	
Boundary layer	YSU PBL scheme			Source term	Ground release (10 m)
Radiation	RRTM for longwave				Cross-sectional area (120 m^2)
	Simple cloud-interactive shortwave radiation scheme				Steady-state unit emission (1 Bq/m^2/s)
Surface scheme	Noah land surface scheme			Dispersion coefficient	Pasquill–Gifford (for rural)
Microphysics	WRF single-moment 3-class scheme				McElroy–Pooler (for urban)
Convection	Kain–Fritsch cumulus scheme			Terrain algorithm	Complex terrain algorithm
				Scavenging coefficient	1×10^{-4}

WRF, weather research and forecasting; CALPUFF, California Puff.

320, 640, 1,200, 2,000, 3,000, and 4,000 m above ground level. Pasquill–Gifford (PG) and McElroy–Pooler dispersion coefficients were used for rural areas and urban areas, respectively, and the complex terrain algorithm of the partial plume path adjustment was applied in this study. We assumed that the radionuclides were absorbed in small particles with an aerodynamic diameter of under 0.95 μm. Accordingly, dry and wet depositions were simulated using particulate characteristics. For the wet deposition, a scavenging coefficient of 1×10^{-4} for particles was used for liquid precipitation.

3. Results and discussion

3.1. Characteristics of the meteorological field at the KJRR site

When using the Gaussian straight line model, the meteorological data at a nuclear facility site become very significant when estimating dispersion characteristics (e.g., frequency, possible area, and direction of high radiation dose). For this reason, the meteorological data should be observed over a long period and thoroughly analyzed. For the KJRR site, based on a 10-minute resolution of the observational data from September 2014 to August 2015, the annual rainfall was 1,078 mm, the mean temperature was 16.5°C, and the frequency of calm wind, defined as below 0.5 m/s, at the KJRR site was 10.8%. The wind speed frequency at 10 m and 65 m above ground at the KJRR site is presented in Fig. 2. The histogram of the wind speed at 10 m above ground was 1.43 ± 0.97 m/s, while at 65 m above ground it was 3.56 ± 2.13. It was found that 79.8% of the wind was under 2.0 m/s and 95.5% was under 5.0 m/s at 10 m, whereas 29.8% of the wind was under 2.0 m/s and 76.4% under 5.0 m/s at 65 m. The wind pattern at the KJRR site is prevailing wind from the northeast (N, NNE: 20.65%) and west (W, WNW: 15.66%) directions. If the wind direction is divided into terrestrial characteristics with land and sea, as depicted in Fig. 1, the frequency of occurrence of land breeze (e.g., SW-NNE) at 10 m height was predominant at 58.2% compared with that for sea breeze (NE-SSW: 31.0%). Furthermore, the frequency of occurrence of wind blowing toward the sea (e.g., SW-NNE) at the effective stack height was also 68.7%. This means that radioactive materials in an unexpected accident would be mainly dispersed to the sea direction, because KJRR is located in the vicinity of the coastline.

Along with wind field and stability, the mixing height is an important input variable with respect to the dispersion of radioactive materials. The mixing height, which is defined as the height of the layer at which turbulence occurs adjacent to the ground, was extracted by WRF–MMIF simulation at the KJRR site for a 1-year period. The seasonal variation of hourly mixing heights is shown in Fig. 3. The average (with standard deviation) estimated mixing heights in spring, summer, fall, and winter were 571 ± 374, 450 ± 259, 452 ± 267, and 372 ± 179 m, respectively. Significant seasonal differences ($p < 0.05$) were not observed. The seasonal variation of simulated mixing heights from the WRF model shows its maximum value in spring and minimum value in winter, representing a range of mixing height between 200 and 1,200 m, which is consistent with the observed characteristics of mixing height over the Korean Peninsula [23]. Also the mixing heights extracted from the WRF–MMIF reflected hourly phenomena well, showing high values in daytime and reduced values at night time.

Extended periods of the meteorological field, over a 1-year period, were sequentially extracted from WRF and MMIF, and field measurements were carried out onsite at KJRR. To estimate the ability of the WRF–MMIF to reproduce the meteorological data, the simulated data were compared with the measurement data at KJRR onsite, especially for wind patterns. Furthermore, to identify the pattern of wind speed and direction around 30-km radius around

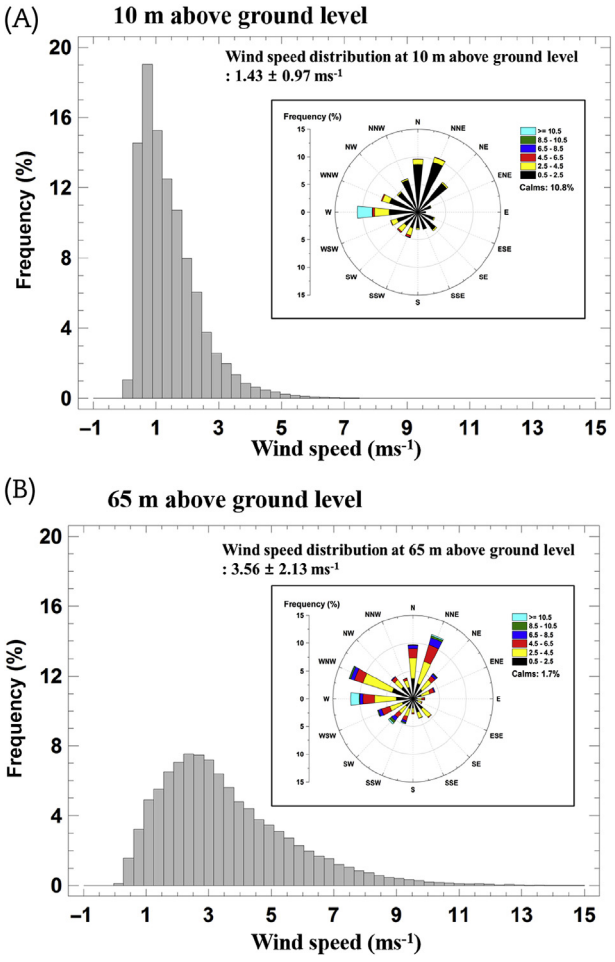

Fig. 2. Frequency of wind speed; (A) At 10 m above ground level, (B) At 65 m above ground level at KJRR site. The wind rose plots are also shown to identify the prevailing wind direction.

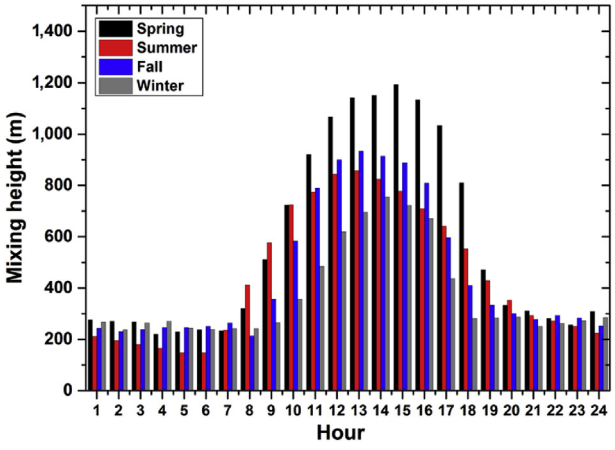

Fig. 3. Hourly variation in mixing height at the KJRR site.

KJRR, the site-specific meteorological data from KMA were also compared with the corresponding points of extracted data obtained by simulation. A comparison of the results at five observation points (refer Fig. 1) are presented as wind rose plots in Fig. 4. The meteorological data, including temperature, humidity, wind

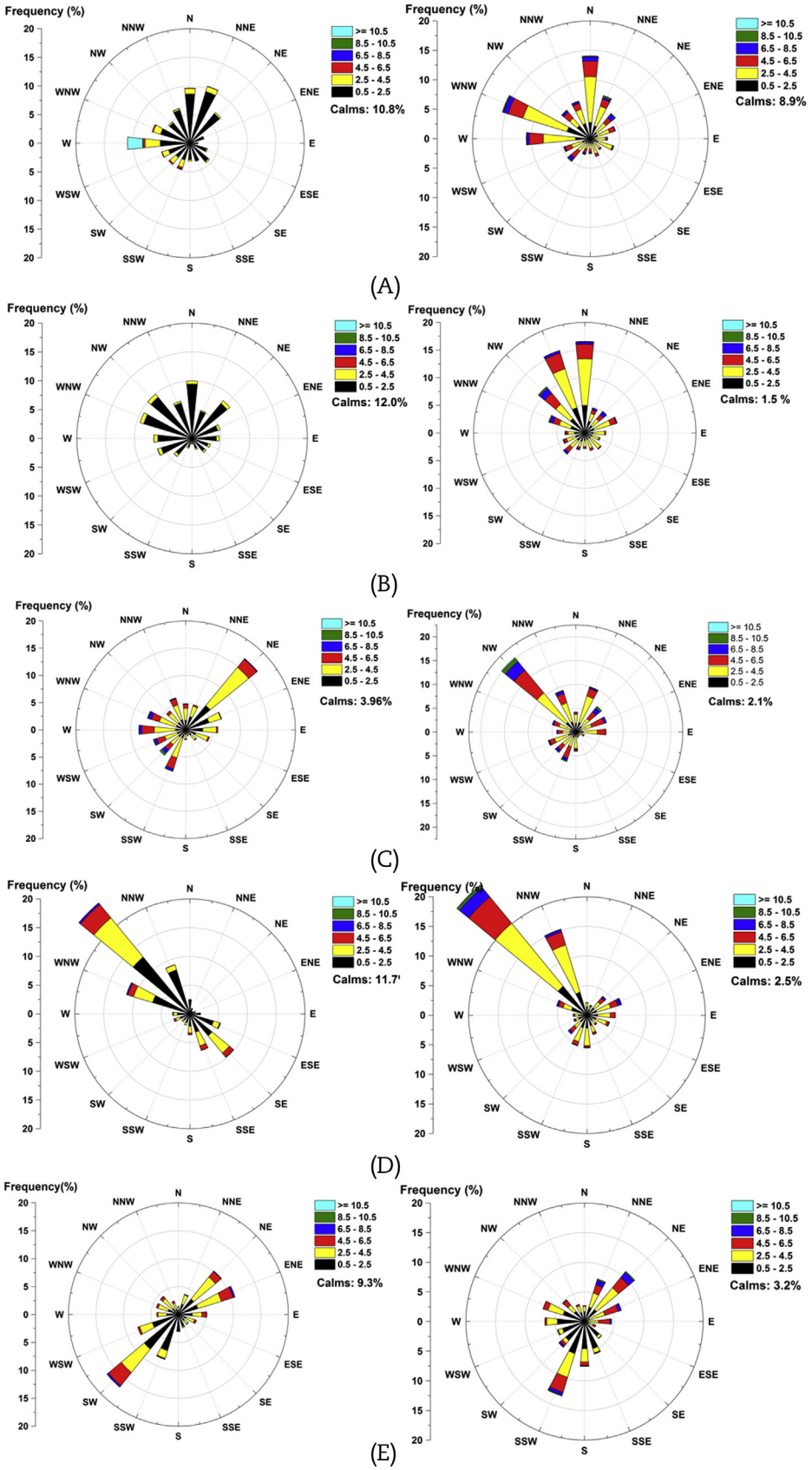

Fig. 4. Wind rose plots extracted from observations (left) and WRF-MMIF (right) at five observation stations; (A) On site, (B) Ulsan, (C) Busan, (D) Kimhae, and (E) Yangsan.

pattern, and precipitation values re-produced by the WRF–MMIF were also compared using statistical approaches. The determination coefficient (R^2), mean bias (MB), normalized mean error (NME), and root mean square error (RMSE) were used to evaluate the consistency at all observation points. The R^2, MB, NME, and RMSE were calculated using the following equations:

$$R^2 = \frac{\overline{\left(Obs - \overline{Obs}\right)\left(Model - \overline{Model}\right)}}{\sigma_o \, \sigma_P} \quad (1)$$

$$\mathrm{MB} = \sum_{1}^{N} \frac{(Model - Obs)}{N} \quad (2)$$

$$\mathrm{NME\%} = \frac{\sum_{1}^{N} |Model - Obs|}{\sum_{1}^{N} (Obs)} \times 100 \quad (3)$$

$$\mathrm{RMSE} = \sqrt{\sum_{1}^{N} \frac{(Model - Obs)^2}{N}} \quad (4)$$

where, *Obs* and *Model* represent the observed and predicted values, respectively; σ_o and σ_p denote the standard deviation of the observed and predicted values, respectively, and N is the number of values analyzed. A determination coefficient close to 1 indicates greater agreement between the observed and predicted values. The MB quantifies the overall systematic bias [e.g., overestimation (MB > 0) or underestimation (MB < 0)], and the RMSE provides information for the distribution of the residuals. As an error estimation method, the RMSE provides good prediction accuracy [24]. As shown in Fig. 4, the prevailing wind direction predicted by the WRF–MMIF simulation corresponded to the observed data for all stations except the Busan site. Overall, this similarity indicates that the dispersion modeling results obtained using prognostic data may compare favorably to those obtained using observation data. Because of the difficulty of representing local wind in a very complex central city flow in the model, differences in the prevailing wind direction were clearly observed at the Busan station.

Table 2 summarizes the statistical analysis for the temperature, humidity, wind speed, and wind direction. Temperature and relative humidity have strong correlation coefficients of 0.93–0.95 and 0.82–0.87 between the predicted and observed data, respectively. The MB for these parameters ranged from 0.70 to 1.35°C and from 1.04% to 1.40% for all stations, respectively. One may conclude that the temperature and relative humidity data predicted by WRF–MMIF were in agreement with the values observed for all stations. The predicted wind speed data shows a moderate determination coefficient of 0.38 at Busan and of 0.64 at Yangsan station. Systematic overestimation, evaluated in terms of NME%, was observed for all stations; it was 52.7% onsite, 46.1% for Ulsan, 72.0% for Busan, 50.8% for Kimhae, and 39.9% for Yangsan. Although this overestimation of wind speed pattern might affect the dispersion of radionuclides in the model output, leading to subsequently underestimated results due to wide dispersion from the source region, using a three-dimensional gridded wind vector still offers notable advantages. Biases and inconsistencies in surface wind speed and direction are usually reported over mountainous and coastal areas when produced by WRF with observation data [25]. However, the model performance can be improved with a finer horizontal resolution grid and multiscale terrain and land use data [26,27]. Indeed, according to Lee et al. (2016), when a sub-grid topography parameterization was applied, the prediction accuracy of the wind speed and direction near the surface also improved [25]. Thus, continuous efforts to simulate a more realistic wind field are required in the WRF simulation for application to dispersion modeling. It should be noted that the wind field patterns at each point for the 1-year period were obviously different. The simulation results from the Gaussian straight line model using the mean wind pattern at the nuclear facility thus do not represent real dispersion characteristics.

Comparison results between observed and predicted precipitation data are shown in Fig. 5. Since the dispersion model (e.g., CALPUFF) calculates the wet deposition with precipitation data, the reproducibility of precipitation from meteorological simulations plays an important role, along with wind field pattern. In a numerical weather prediction system, which is constructed to simulate atmospheric phenomena during a long-term period, precipitation at small spatial scales with varying prediction time is the most difficult variable to simulate due to limited information. Furthermore, because the precipitation data reproduced from WRF and MMIF in this study spatially represent area-average values, comparison with measurement data at a point within a complex terrain region could lead to systematic and representativeness error [28]. As shown in Fig. 5, the determination coefficients between observed and predicted values are 0.62 for Ulsan, 0.79 for Busan, 0.65 for Kimhae, and 0.58 for Yangsan station. Based on these comparison results, rainfall data reproduced from WRF and MMIF in this study were in moderate agreement with the values observed for all stations.

3.2. Simulated dispersion (χ/Q) and deposition (D/Q) factors

The inhaled dose of radioactive particulate (and gas) in the ground-level layer and public exposure to ground deposited particulates should be considered while evaluating accidental releases. For this reason, the ground-level concentration and the deposition of radioactive materials were computed independently under all meteorological conditions from September 2014 to August 2015. Because the amount released from the facility in an unexpected severe accident might be difficult to accurately predict,

Table 2
Statistical summary for temperature, wind speed, and direction between observed and predicted values.

Station	Temperature (°C)				Relative humidity (%)				Wind speed (m/s)				Wind direction (degree)	
	R^2	MB	NME%	RMSE	R^2	MB	NME%	RMSE	R^2	MB	NME%	RMSE	MB	RMSE
Onsite	0.94	0.70	12.6	2.35	0.86	1.34	15.3	2.31	0.48	1.1	52.7	2.6	10.5	67.2
Ulsan	0.94	1.01	14.0	2.57	0.82	1.19	12.2	1.64	0.54	1.0	46.1	1.9	13.0	51.3
Busan	0.94	0.99	12.5	2.36	0.80	1.40	14.1	2.20	0.38	2.1	72.0	3.0	51.4	105.9
Kimhae	0.95	1.00	12.8	2.37	0.84	1.21	12.9	1.95	0.51	0.9	50.8	2.1	9.0	68.3
Yangsan	0.93	1.35	15.6	2.86	0.87	1.04	11.1	1.52	0.64	0.5	39.9	1.6	7.6	51.7

MB, mean bias; NME, normalized mean error; RMSE, root mean square error; R^2, determination coefficient.

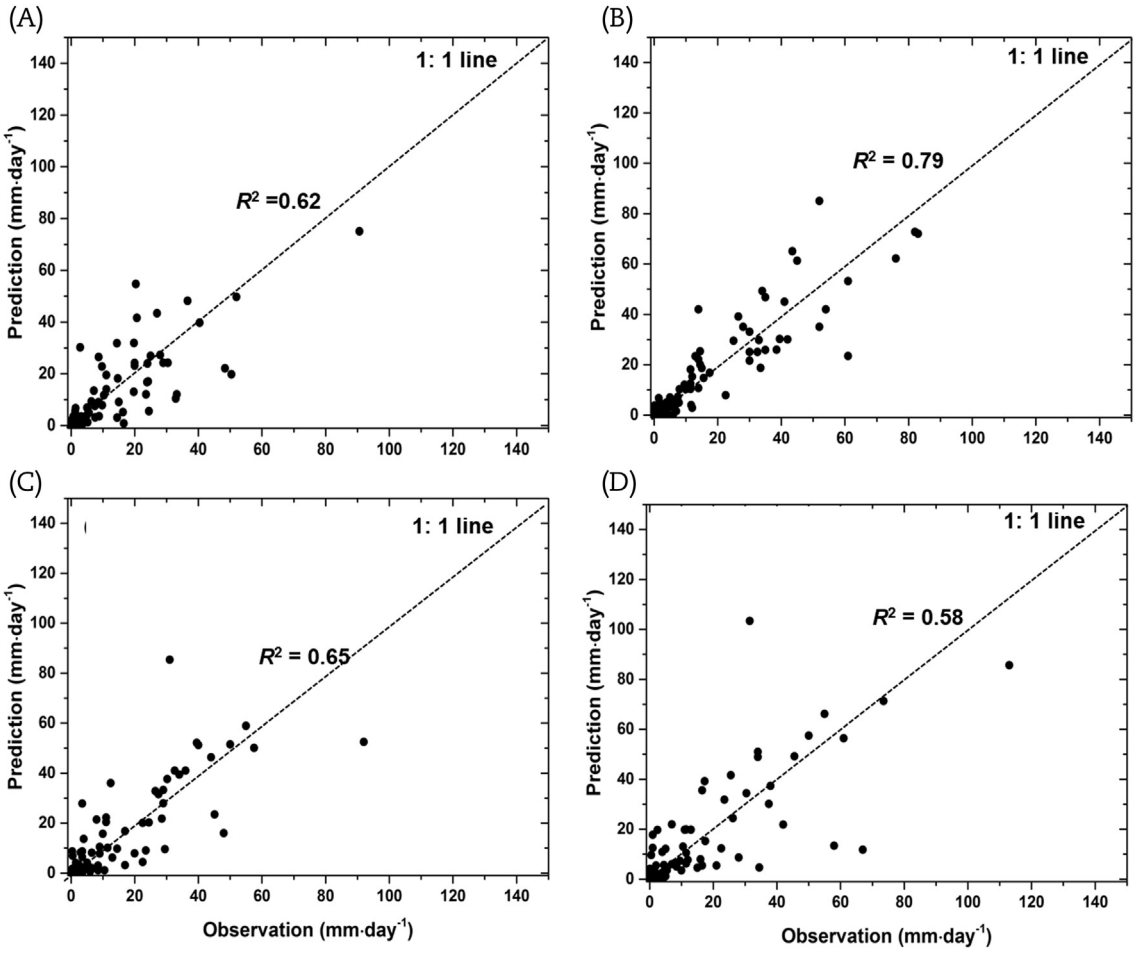

Fig. 5. Two-dimensional scatterplots for precipitation between observed and predicted values; A) Ulsan, (B) Busan, (C) Kimhae, and (D) Yangsan.

the simulation focused on an evaluation of the dispersion direction, the dilution factor, and the possibility of a high dose of radiation in the study area. The dispersion (χ/Q) and deposition (D/Q) factors, which correspond to the average concentration or deposition by using a unit release rate (Q), were calculated using three dimensional gridded meteorological data over a 1-year period. This means that the dispersed concentration in air or the amount deposited around the nuclear facility can be directly estimated by the product of those factors and the release rate. A continuous unit emission rate (1.0 Bq/m^2/s) for 1 year was used to evaluate hourly χ/Q and D/Q at the 17,161 nodes. The cross-sectional area of ground release is assumed to be 120 m^2. The seasonal variation of wind pattern at the KJRR site is presented in Fig. 6. The average and 95th percentile values of hourly χ/Q and D/Q data at each node for the 1-year period are presented in Figs. 7 and 8, respectively. The diurnal variation of χ/Q divided into day and night times is also provided with wind rose plots in Fig. 9.

As shown in Figs. 7 and 8, the average and 95th percentile values of 8,760 hourly values of χ/Q and D/Q at each node indicate that the dispersion of radioactive materials released from KJRR mainly depends on the wind field patterns. Heavy contamination in the vicinity of KJRR was observed; the χ/Q values at up to 50 km distance from the source dramatically decreased (by more than 10^6 orders of magnitude). The prevailing land breeze in the study area resulted in relatively higher χ/Q values in the off-shore sectors. All of the χ/Q values in the SE sector (E, ESE, SE, and SSE directions) and SW sector (SW, SSW, and S directions) were 1.9–3.2 times higher than those in the NW sector (NNW, NW, WNW, and W directions). In particular, at 20 km (e.g., the emergency planning zone), the former were 2.6 and 2.8 times higher than the latter, respectively. For the spatial distribution of D/Q, there was also heavy contamination in vicinity of KJRR. However, the area, highly contaminated by wet deposition of emitted radionuclides, was relatively narrow and D/Q values in the south and west regions from the KJRR had values rather higher than those in off-shore sectors. These results reflect that the wet deposition of pollutants was mainly affected by precipitation and that winds prevailed from the southeastern and south during rain in the summer season. From a comparison of the distribution patterns of χ/Q and D/Q on a seasonal basis, significant seasonal differences between the summer and winter seasons were observed for both values. Because the wind pattern was prevailing toward the north-west in summer, the possibility of relatively higher χ/Q and D/Q in the land area increased compared to other seasons.

As shown in Fig. 9, differences in the dispersion pattern between day and night times were also observed. The results indicate relatively higher χ/Q inland in the day time and relatively lower values at night time. These patterns can be explained by the fact that the meteorology (especially, wind direction and speed) is affected by thermal interactions between the mountains and the sea. However, relatively higher values at night time were shown at the vicinity of the release point due to the relatively lower mixing layers and stagnation of air flow.

Lutman et al. (2004) pointed out that the conventional Gaussian type dispersion models for radiological assessment are appropriate for predicting long-range dispersion of continuous releases. Since

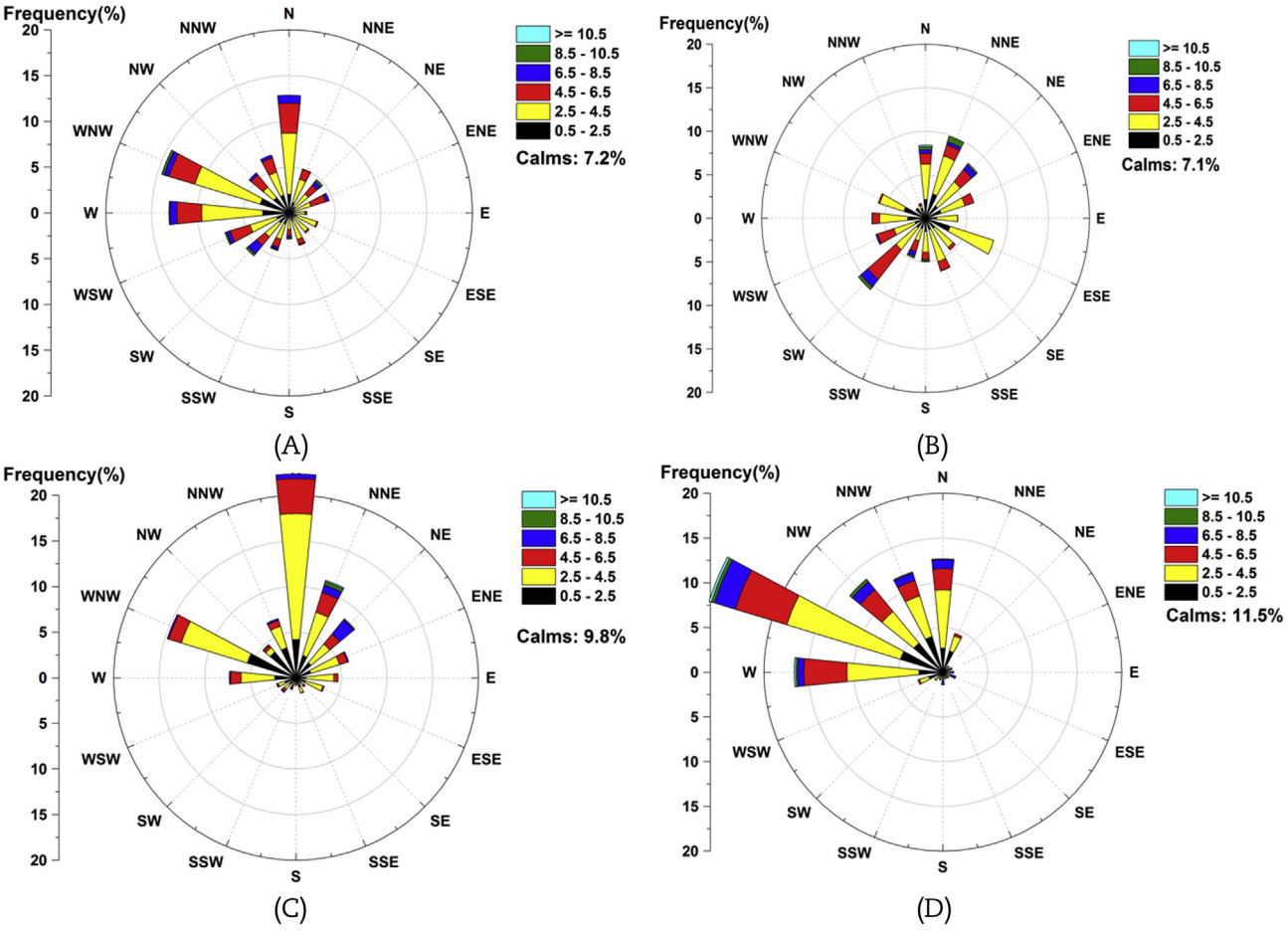

Fig. 6. Wind rose plots extracted from WRF-MMIF with seasonal basis; (A) Spring, (B) Summer, (C) Fall, and (D) Winter.

these models are simple to use and appear to overestimate environmental concentrations, they are widely used to estimate air dispersion characteristics, although the Lagrangian dispersion model can provide more complete and realistic dispersion characteristics [29]. Accordingly, the PAVAN model, one of the conventional Gaussian type dispersion models which estimates ground level concentrations downwind of accidental radionuclide releases from nuclear facilities into the atmosphere, was also applied in this study. The joint frequency function of wind speed and direction for 16 sectors according to atmospheric stability class at the KJRR site were reproduced using the WRF–MMIF simulation output. The wind speed class for the PAVAN simulation was divided into 11 levels (1, 1.5, 2, 3, 4, 5, 6, 8, 10, and 14.13 m/s), including calm wind. The ground emission option and PG diffusion parameter were used for dispersion. Site-specific terrain correction factors were not applied. χ/Q values were calculated for distances from 400 m to 50,000 m and compared with the 95th percentile values of hourly χ/Q from CALPUFF. The ratios (PAVAN/CALPUFF) at the 16 sectors are shown in Table 3. Note that the dry and wet deposition schemes could not be applied in PAVAN. However, for a comprehensive comparison including a consideration of the limitations between the two models, the model outputs were directly compared. The average (with range) ratio for all sectors within 1 km was 0.9 (0.5–2.0). However, for the sectors beyond 5 km, there is a greater divergence, by a factor of 0.9–13.8 with an average of 5.2, between the values from both models. The slightly lower values of PAVAN in vicinity of KJRR reflect the fact that this model could not simulate wake effects by which radionuclides are deflected and advected over the complex terrain. However, because the dry and wet deposition scheme could not be applied in PAVAN, as it was applied in CALPUFF, the radionuclides emitted from the source consistently dispersed and diffused along the centerline. For this reason, the values calculated using PAVAN are overestimated for sectors beyond 5 km. This overestimation implies that a Gaussian type dispersion model (e.g., PAVAN) leads to conservative dose for preliminary safety analysis estimates. Nevertheless, these results do not necessarily reflect the need to seriously change the facility design because, finally, the resulting conservative dose has a very low level. To overcome these disadvantages, Till et al. (2014) proposed the use of a Lagrangian dispersion model such as CALPUFF for deterministic safety analyses and Gaussian type dispersion models for probabilistic safety analyses [14].

According to a study of ^{137}Cs dispersion characteristics when hypothetically released from the Kori nuclear power plant (NPP) near KJRR [30], a comprehensive assessment of weather, geography, topography, and emission conditions is required for the emergency response in this study area. Thus, to identify meteorological conditions for the cases of relatively higher χ/Q, we examined hourly χ/Q distribution at five discrete receptors; (a) Busan, (b) Ulsan, (c) Kimhae, (d) Miyrang and (e) the sea area. As threshold criteria, the 95th percentile concentrations were employed. The meteorological conditions of wind speed and direction, mixing height, and PG stability at KJRR were analyzed in terms of frequency and are provided in Table 4. The relatively higher χ/Q at specific receptors mainly depends on the wind direction. However, under moderately unstable conditions and wind blowing from N and NNW with relatively low wind speed (1.0–2.0 m/s) at the KJRR site, the possibility of a maximum dose to the public was higher when

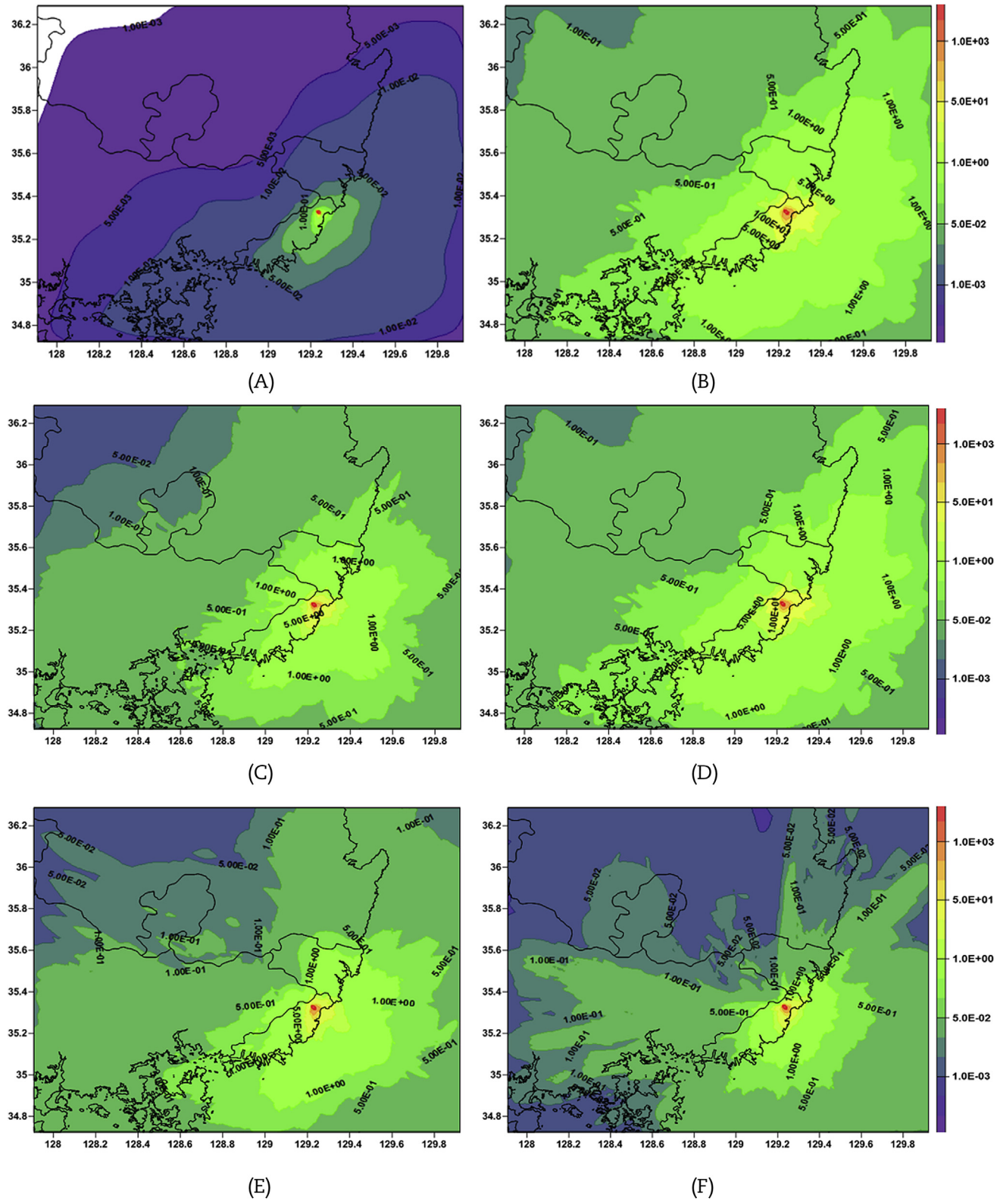

Fig. 7. Spatial distribution of hourly dispersion factor (χ/Q). All values expressed are multiplied by 10^6; (A) annual average of χ/Q, 95th percentile of χ/Q in B) All period, (C) Spring, (D) Summer, (E) Fall, and (F) Winter.

Busan city, which is located in the S and SSW part of KJRR site, was chosen as the receptor. As shown in Fig. 4, winds blowing from N and NNE as well as from W prevail at the KJRR site. Thus, when westerly winds are dominant at the KJRR site, radionuclides are supposed to be dispersed towards the sea. Meanwhile, winds blowing from N and NNW having relatively low wind speeds (1.0–2.0 m/s), which could enhance the chance of radionuclides residing near Busan by converging winds blowing from N and NNE

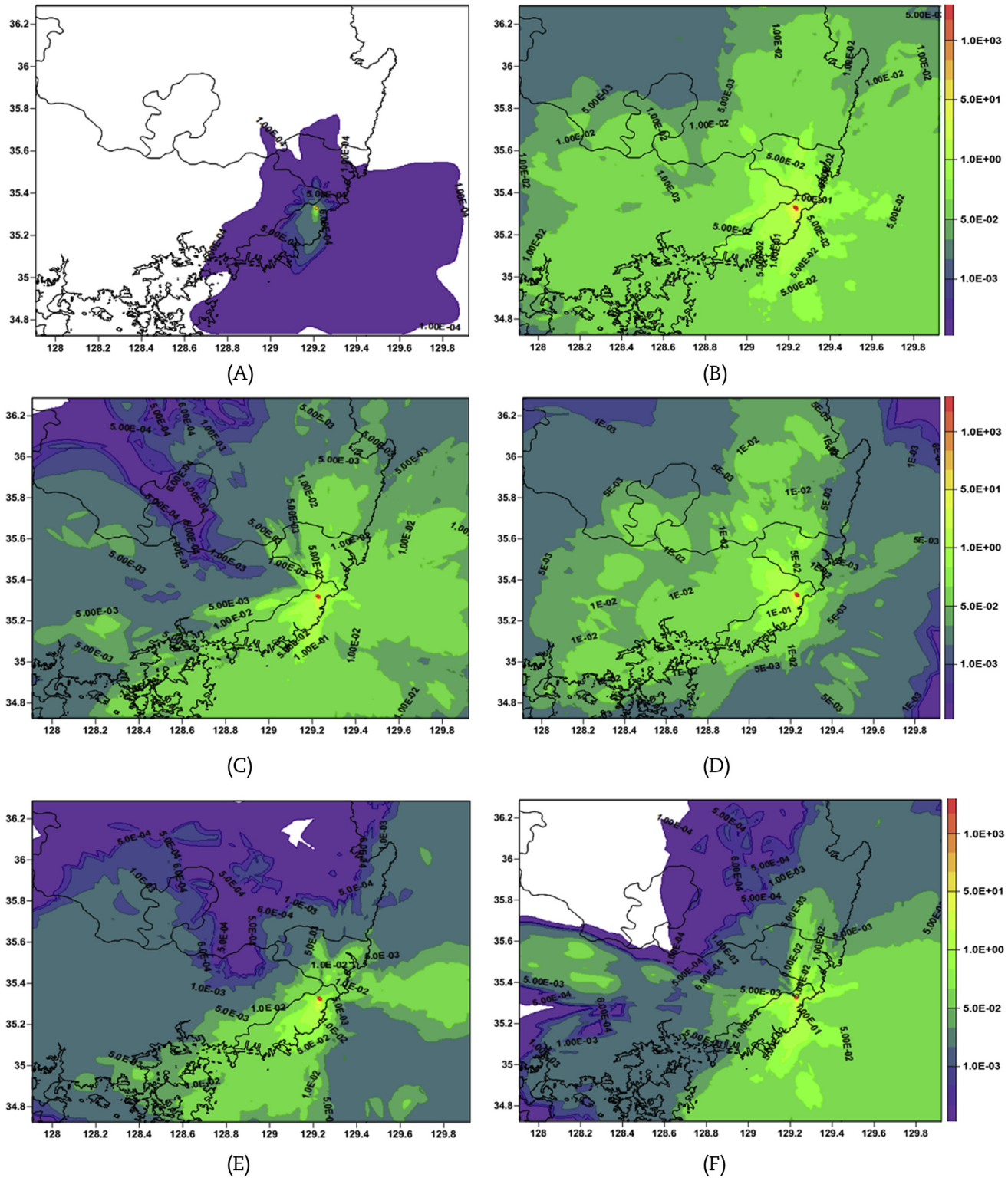

Fig. 8. Spatial distribution of hourly deposition factor (D/Q). All values expressed are multiplied by 10^6; (A) annual average of D/Q, 95th percentile of D/Q in (B) All period, (C) Spring, (D) Summer, (E) Fall, and (F) Winter.

at the Busan site. In addition, radionuclides are not dispersed well during the night time, because the vertical structure of the atmosphere is stable and wind speed is low (see Table 4). This atmospheric condition also results in radionuclides stagnating near the S and SSW parts of the KJRR site, where the Busan site is located.

4. Conclusion

In this study, we attempted to characterize the atmospheric dispersion and deposition of radioactive materials released by an unexpected incident at KJRR. In this study, the WRF–

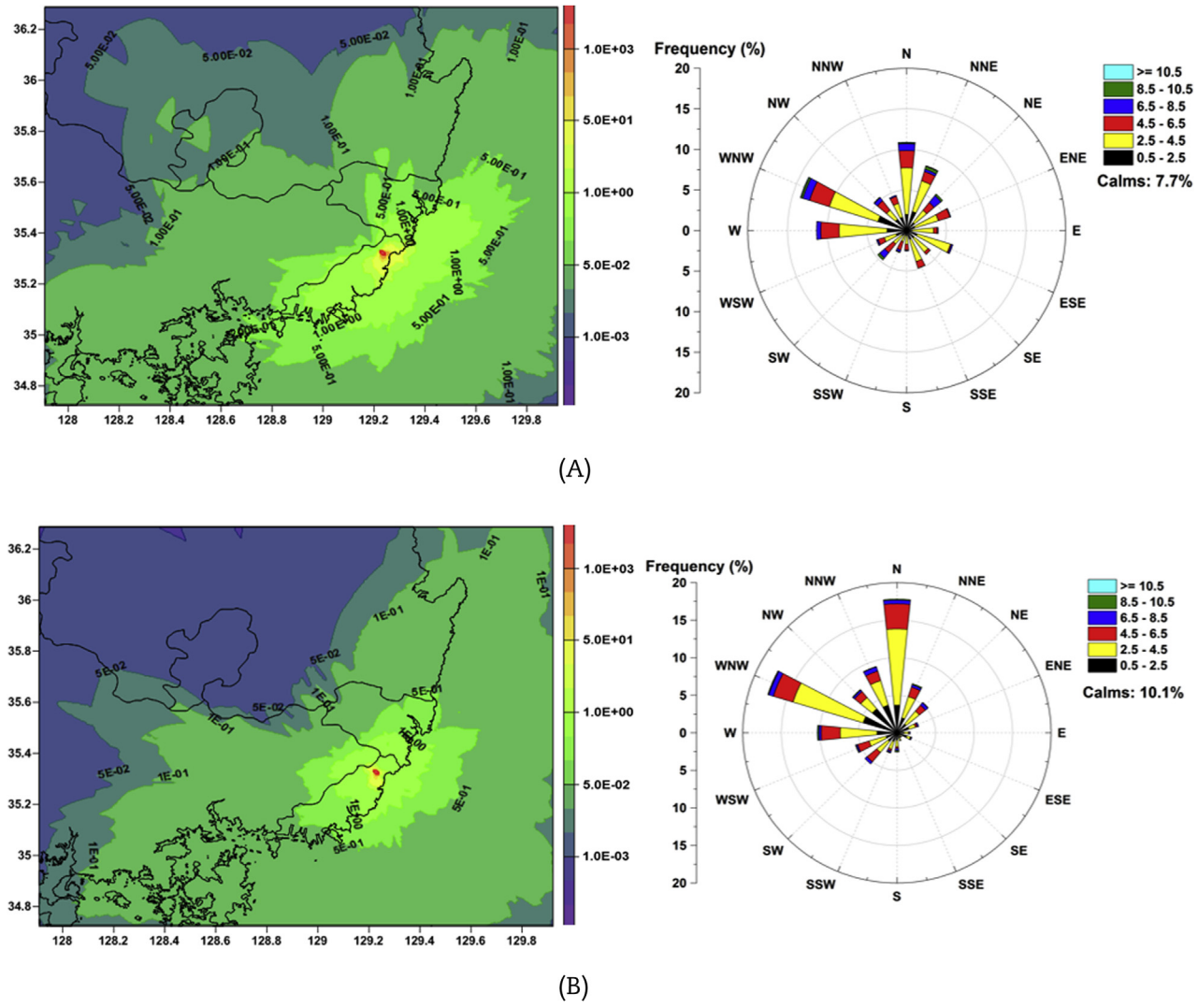

Fig. 9. Diurnal variation of χ /Q and wind pattern. All values expressed are multiplied by 10^6; (A) Day time, and (B) Night time.

Table 3
Comparison results of 95th percentile highest hourly χ/Q values calculated by PAVAN and CALPUFF. The values in this table express the ratio of PAVAN and CALPUFF.

Sector	Distance from KJRR (km)								
	0.4	0.8	1	5	10	20	30	40	50
N	0.9	0.7	0.9	1.5	4.4	3.2	3.8	6.0	8.6
NNE	1.2	0.8	0.8	2.7	3.4	3.7	3.9	5.5	6.1
NE	1.3	0.9	1.0	2.6	4.8	3.5	4.0	4.0	4.3
ENE	0.9	0.6	0.7	2.5	2.7	3.2	4.7	5.4	6.8
E	1.2	0.7	0.7	1.8	3.1	4.2	5.9	6.1	8.0
ESE	1.2	0.8	0.8	1.8	2.9	4.9	7.4	9.3	13.8
SE	0.9	0.6	0.9	2.6	4.1	4.0	5.4	7.6	10.0
SSE	1.0	0.6	0.8	1.6	4.9	6.3	7.5	8.1	9.7
S	1.3	0.8	0.8	1.4	3.7	6.3	7.7	8.6	10.8
SSW	1.0	0.8	0.9	3.3	4.7	6.6	6.7	6.7	8.2
SW	2.0	1.2	1.4	5.0	6.5	7.7	8.9	8.4	8.3
WSW	1.4	0.8	0.7	2.4	2.7	3.1	2.8	3.5	4.0
W	0.9	0.5	0.7	0.9	2.7	2.2	2.6	3.7	3.7
WNW	0.9	0.7	0.9	1.7	3.0	3.5	5.0	5.2	4.8
NW	0.9	0.7	0.9	2.3	3.4	4.8	8.5	11.2	12.3
NNW	0.8	0.6	1.0	3.0	4.4	5.0	5.2	7.7	10.3

KJRR, Ki-Jang research reactor; CALPUFF, California Puff.

MMIF–CALPUFF model system was used to produce high-resolution meteorological fields and to estimate the dispersion of radioactive materials.

Based on a measurement period of 1 year at the KJRR site, the annual average wind speed at 10 m above ground was determined to be 1.43 ± 0.97 m/s, while at 65 m above ground it was 3.56 ± 2.13. The wind pattern at the KJRR site is prevailing from the northeast (N, NNE: 20.65%) and west (W, WNW: 15.66%) directions. The frequency of occurrence of land breeze (e.g., SW-NNE) at 10 m height was predominant at 58.2% compared to that for sea breezes (NE-SSW: 31.0%). From a statistical comparison between the meteorological model outputs from WRF and the field measurement data in the study area, one may conclude that the temperature and relative humidity data predicted by WRF–MMIF are in agreement with the observed data. For wind speed, the predicted wind speed data were slightly overestimated at all stations. Although this trend might affect the model output, leading to subsequently underestimated results, using a three-dimensional gridded wind vector still offers notable advantages.

The main dispersion direction and the possibility of a high dose of radiation were simulated using a three-dimensional gridded

Table 4
Meteorological conditions for hours observed beyond 95th percentile highest χ/Q.

Receptor site	Receptors			Meteorological condition				
	Direction	Distance (km)	Criteria[a]	Hour	Wind speed (m/s)	Wind direction	Mixing height (m)	PG stability
Busan	SSW	20	5.71	02–06	1.0–2.0	N, NNW	<200	B, C
Ulsan	NE	20	2.74	12–20	2.0–4.0	SSW, S, SSE	<200	A, B
Kimhae	WSW	25	2.28	18–24	1.5–3.5	NE, ENE	<600	B
Miryang	NW	45	0.43	2–6, 16–20	1.0–3.5	ESW, SE, SSE	<400	A, B
On sea	SE	10	7.61	02–10	2.5–3.5	WNW	<200	C

PG, Pasquill–Gifford.
[a] 95th percentile highest χ/Q at receptor (multiplied by 10^6).

meteorological model output. Heavy contamination in the vicinity of KJRR was observed, and the prevailing land breeze in the study area resulted in relatively higher concentrations and deposition in the sea area sectors. Based on a comparison of the results from PAVAN and CALPUFF, the average (with range) ratio for all sectors within 1 km was 0.9 (0.5–2.0). However, for the sectors beyond 5 km, there was a greater divergence, by a factor of 0.9–13.8, with an average of 5.2, between the values from these two models. Therefore, based on the results of this study, the Gaussian type dispersion models (e.g., PAVAN), which lead to a conservative dose for preliminary safety analysis estimates, can result in unnecessary and costly facility design changes. Under moderately unstable conditions and with wind blowing from the N and NNW at a relatively low wind speed (1.0–2.0 m/s), the possibility of public exposure to a maximum dose was higher in the Busan city area in the south-west direction from KJRR.

In terms of applicability and to evaluate realistic dispersion characteristics, the dispersion assessment system using WRF–MMIF–CALPUFF in the present work is useful for evaluating the characteristics of regional scale atmospheric dispersion around KJRR.

Conflicts of interest

All authors have no conflicts of interest to declare.

References

[1] IAEA, Generic Procedures for Assessment and Response during a Radiological Emergency, IAEA-TECDOC-1162, 2000.
[2] Roland Draxler, Dèlia Arnold, Masamichi Chino, Stefano Galmarini, Matthew Hort, Andrew Jones, Susan Leadbetter, Alain Malo, Christian Maurer, Glenn Rolph, Kazuo Saito, René Servranckx, Toshiki Shimbori, Efisio Solazzo, Gerhard Wotawa, World Meteorological Organization's model simulations of the radionuclide dispersion and deposition from the Fukushima Daiichi nuclear power plant accident, J. Environ. Radioact. 139 (2015) 172–184.
[3] G. Katata, M. Ota, H. Terada, M. Chino, H. Nagai, Atmospheric discharge and dispersion of radionuclides during the Fukushima Dai-ichi Nuclear Power Plant accident. Part I: source term estimation and local-scale atmospheric dispersion in early phase of the accident, J. Environ. Radioact. 109 (2012) 103–113.
[4] M. Chino, H. Nakayama, H. Nagai, H. Terada, G. Katata, H. Yamazawa, Preliminary estimation of release amounts of ^{131}I and ^{137}Cs accidentally discharged from the Fukushima Daiichi nuclear power plant into atmosphere, J. Nucl. Sci. Technol. 48 (2011) 1129–1134.
[5] S.U. Park, I.H. Lee, J.W. Ju, S.J. Joo, Estimation of radionuclide (^{137}Cs) emission rates from a nuclear power plant accident using the Lagrangian Particle Dispersion Model (LPDM), J. Environ. Radioact 162–163 (2016) 258–262.
[6] C.V. Srinivas, R. Venkatesan, R. Baskaran, V. Rajagopal, B. Venkatraman, Regional scale atmospheric dispersion simulation of accidental releases of radionuclides from Fukushima Dai-ichi reactor, Atmos. Environ. 61 (2012) 66–84.
[7] I. Korsakissok, A. Mathieu, D. Didier, Atmospheric dispersion and ground deposition induced by the Fukushima Nuclear Power Plant accident: a local-scale simulation and sensitivity study, Atmos. Environ. 70 (2013) 267–279.
[8] A.S. Rood, A.J. Sondrup, P.D. Ritter, Quantitative evaluation of an air-monitoring network using atmospheric transport modeling and frequency of detection methods, Health Phys. 110 (2016) 311–327.
[9] U.S. Nuclear Regulatory Commission, XOQDOQ: Computer Program for Meteorological Evaluation of Routine Effluent Releases at Nuclear Power Stations, NUREG-0324, 1982.
[10] U.S. Nuclear Regulatory Commission, PAVAN: An Atmospheric Dispersion Program for Evaluating Design Basis Accidental Releases of Radioactive Materials from Nuclear Stations, NUREG/CR-2858, 1982.
[11] USEPA, Clarification of Regulatory Status of CALPUFF for Near-field Applications, U.S. Environmental Protection Agency, Research Triangle Park, NC, 2008.
[12] A.S. Rood, Performance evaluation of AERMOD, CALPUFF, and legacy air dispersion models using the Winter Validation Tracer Study dataset, Atmos. Environ. 89 (2014) 707–720.
[13] J.K. Lee, J.C. Kim, K.J. Lee, M. Belorid, P.A. Beeley, J.I. Yun, Assessment of wind characteristics and atmospheric dispersion modeling of ^{137}Cs on the Barakah NPP area in the UAE, Nucl. Eng. Technol. 46 (2014) 557–568.
[14] J.E. Till, A.S. Rood, C.D. Garzon, R.H. Lagdon Jr., Comparison of the MACCS2 atmospheric transport model with Lagrangian puff models as applied to deterministic and probabilistic safety analysis, Health Phys. 107 (2014) 213–230.
[15] G.P. Ronchin, F. Campi, A.A. Porta, Incineration of urban solid wastes containing radioactive sources, Radiat. Meas. 46 (2011) 133–140.
[16] R.C. Gilliam, J.E. Pleim, Performance assessment of new land surface and planetary boundary layer physics in the WRF-ARW, J. Appl. Meteorol. Clim. 49 (2010) 760–774.
[17] W.C. Skamarock, J.B. Klemp, J. Dudhia, D.O. Gill, D.M. Barker, M.G. Duda, X.Y. Huang, W. Wang, J.G. Powers, A Description of the Advanced Research WRF Version 3, NCAR, Boulder, 2008.
[18] J.L. Case, W.L. Crosson, S.V. Kumar, W.M. Lapenta, C.D. Perter-Lidard, Impacts of high resolution land surface initialization in regional sensible weather forecasts from the WRF model, J. Hydrometeorol. 9 (2009) 1249–1266.
[19] F. Chen, K.W. Manning, M.A. Lemone, S.B. Trier, J.G. Allfieri, R. Roberts, M. Tewari, D. Niyogi, T.W. Horst, S.P. Oncley, J.B. Basara, P.D. Blanken, Description and evaluation of the characteristics of the NCAR high-resolution land data assimilation system, J. Appl. Meteorol. 46 (2007) 694–713.
[20] F. Zhang, Y. Weng, J.F. Gamache, F.D. Marks, Performance of convection-permitting hurricane initialization and prediction during 2008–2010 with ensemble data assimilation of inner-core airborne Doppler radar observations, Geophys. Res. Lett. 38 (2011) L15810.
[21] J.S. Scire, D.G. Strimaitis, R.J. Yamarito, A User's Guide for the CALPUFF Dispersion Model (Version 5), Earth Tech, Concord, MA, 1999.
[22] B. Brashers, C. Emery, The Mesoscale Model Interface Program (MMIF) Version 3.0, ENVIRON International Co, CA, 2013.
[23] S.J. Lee, J. Lee, S.J. Greybush, M. Kang, J. Kim, Spatial and temporal variation in PBL height over the Korean Peninsula in the KMA operational regional model, Adv. Meteorol. (2013) 1–16. Article ID 381630.
[24] EPA, Guidance on the Use of Models and Other Analyses for Demonstrating Attainment of Air Quality Goals for Ozone, PM2.5 and Regional Haze, 2007.
[25] J.H. Lee, H.H. Shin, S.Y. Hong, P.A. Jimenez, J. Dudhia, J.K. Hong, Impacts of subgrid-scale orography parameterization on simulated surface layer wind and monsoonal precipitation in the high-resolution WRF model, J. Geophys. Res. Atmos. 120 (2016) 644–653.
[26] J.H. Ha, D.K. Lee, Effect of length scale tuning of background error in WRF-3DVAR system on assimilation of high-resolution surface data for heavy rainfall simulation, Adv. Atmos. Sci. 29 (2012) 1142–1158.
[27] D.H. Kim, H.W. Lee, S.H. Lee, Evaluation of wind resource using numerically optimized data in the Southwestern Korea Peninsula, Asia-Pac. J. Atmos. Sci. 46 (2010) 393–403.
[28] X. Xiaoduo, X. Li, Comparison of downscaled precipitation data over a mountainous watershed: a case study in the Heihe river basin, J. Hydrometeorol. 15 (2014) 1560–1574.
[29] E.R. Lutman, S.R. Jones, R.A. Hill, P. MacDonald, B. Lambers, Comparison between the predictions of a Gaussian plume model and a Lagrangian particle dispersion model for annual average calculations of long-range dispersion of radionuclides, J. Environ. Radioact. 75 (2004) 339–355.
[30] H.Y. An, Y.H. Kang, S.K. Song, Y.K. Kim, Atmospheric dispersion characteristics of radioactive materials according to the local weather and emission conditions, J. Radiat. Prot. Res. 41 (2016) 315–327.